

PORE-SCALE SIMULATION OF MAGNETOSOLUTAL MICROCONVECTION IN FERROFLUID SATURATED POROUS STRUCTURES

D. Zablotzky, E. Blums

*Institute of Physics, University of Latvia, 32 Miera str., Salaspils, LV-2169, Latvia
e-Mail: dmitrijs.zablockis@gmail.com*

We consider an idealized model of ferrofluid saturated porous medium composed of microscale non-magnetic inclusions with simple geometry. The application of a uniform magnetic field induces a complicated pattern of internal demagnetizing fields owing to the difference in magnetic permeability. In turn, the imbalance of ferroparticle concentration is created by non-uniform heating and associated colloidal thermophoresis. Numerical simulations of magnetosolutal microconvection show significant intensification of pore-scale mixing and appearance of solvent flux in the direction of temperature gradient.

Introduction. Ferrofluids – colloidal solutions of magnetic nanoparticles – exhibit a pronounced Soret effect, i.e. colloidal thermophoresis. The influence of magnetic field on the drift of colloidal particles attracts interest as a means of control and intensification of mass transport in these media. While theory predicts that in bulk solutions the direct dependence of molecular mass transport coefficients on the uniform magnetic field is weak [1–3], specific microconvective phenomena, i.e. magnetic solutal microconvection, may appear [4–5] causing significant intensification of mass transfer. Recent experimental evidence [6–7] suggests that magnetic phenomena are also quite significant in porous environments or membranes resulting in considerable attenuation of the thermophoretic separation due to enhanced mixing. It is hypothesized that similar magnetic microconvection may be partially responsible for this effect [8].

When a magnetic field is applied to a ferrofluid saturated porous medium, the jump of magnetic permeability across the boundary of non-magnetic inclusions may cause the appearance of significant gradients of internal magnetic field in the vicinity of the interface. A system of such inclusions thus forms a markedly non-uniform internal magnetic field within the porous environment. In turn, in the conditions of non-uniform heating, the strong colloidal thermophoresis initiates the formation of corresponding gradients of ferroparticle concentration. Both the appearance of spatial non-homogeneity of the distribution of the dispersed magnetic phase and the internal magnetic field contribute to the formation of the associated non-potential magnetosolutal buoyant force, which may entrain the ferrofluid and create pore-scale magnetosolutal microconvection. Apart from pore-scale microconvective circulations [8–9], the formation of integral flow is possible in the vicinity of the inclusions [8].

Here we report preliminary results of numerical simulations of pore-scale magnetosolutal microconvection in a geometrically simple model of porous media. We create a 1D arrangement of non-magnetic microscale cylinders immersed in a ferrofluid (Fig. 1). Placing the cylinders periodically on a regular lattice with a period l every other row is shifted vertically by half the period, as shown in Fig. 1. Assuming the radius of the cylinders as the length scale, the porosity of the system is $\varepsilon = 1 - \pi/l^2$, where the period l is expressed in units of the radius of the cylinder. A temperature gradient is applied across the structure and a uniform external magnetic field is imposed in the same direction.

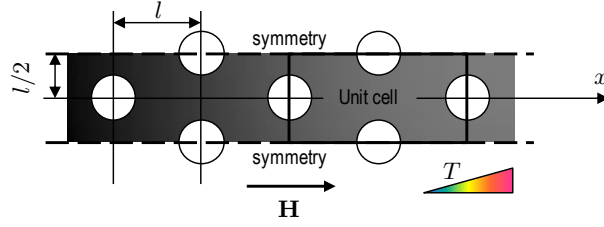


Fig. 1. Scheme of the arrangement – non-magnetic cylindrical elements immersed in a ferrofluid, temperature gradient and magnetic field are applied across the porous structure.

1. Magnetic microconvection. The magnetic force density acting on the ferrofluid due to the magnetic field is expressed by the Kelvin body force term $\mathbf{F} = \mu_0(\mathbf{M}\nabla)\mathbf{H}$ [10], with \mathbf{M} being the magnetization of the ferrofluid, μ_0 the vacuum permeability and \mathbf{H} the magnetic field. Assuming $\mathbf{M} = \chi(c)\mathbf{H}$, where $\chi(c)$ is the magnetic susceptibility at a given mass concentration of magnetic nanoparticles and magnetic field, and with the linear relationship for the magnetic susceptibility $\chi(c) = \chi_0(1 + \chi_c\Delta c)$, where $\Delta c = c - c_0$, c_0 is a reference mass concentration, $\chi_c = 1/c_0$ and χ_0 is the susceptibility at reference parameters, the non-potential part of the force density becomes

$$\mathbf{F} = \mu_0\chi_0\chi_c\Delta cH_0\nabla[(\mathbf{h} + \Delta\mathbf{H}/(2H_0))\Delta\mathbf{H}]$$

with $\Delta\mathbf{H} = \mathbf{H} - \mathbf{H}_0$, $\mathbf{H}_0 = H_0\mathbf{h}$ being a reference magnetic field, \mathbf{h} is the unit vector. Thus, the variation of the ferroparticle concentration and magnetic field can produce magnetic convection in ferrocolloid.

The diffusive dynamics of colloidal nanoparticles is very slow and relevant only on submillimetre lengthscales. In turn, the Schmidt number $Sc = \eta(\rho D)^{-1}$ (where η and ρ are the viscosity and density of ferrocolloid, D the diffusivity of ferroparticles) expresses the ratio of momentum and mass diffusivities and is of the order $10^4 - 10^5$. The magnetosolutal microconvection then is a creeping convection. Introducing characteristic scales for the length L (equal to the radius of the cylindrical inclusion), time L^2D^{-1} , magnetic field $\overline{\Delta H}$, concentration perturbation $\overline{\Delta c}$, the dynamics of ferrocolloid is described by the dimensionless Stokes equation

$$-\nabla p + \Delta\mathbf{u} + \text{Rm}_c\nabla[(\mathbf{h} + r_H\delta\mathbf{H})\delta\mathbf{H}] = 0 \quad (1)$$

and the continuity condition $\nabla \cdot \mathbf{u} = 0$. Here $r_h = \overline{\Delta H}/(2H_0)$ typically does not exceed 5% and is disregarded. The magnetosolutal Rayleigh number is

$$\text{Rm}_c = \mu_0\chi_0\chi_cH_0L^2(\eta D)^{-1}\overline{\Delta c}\overline{\Delta H}.$$

We use overbars to denote the characteristic scales of the concentration $\overline{\Delta c}$, magnetic field $\overline{\Delta H}$ and the temperature $\overline{\Delta T}$ to distinguish these definitions from the deviations of the corresponding quantities from the reference values or the application of the Laplacian operator. The exact values of the corresponding characteristic scales will be given further in the text.

In a non-isothermal ferrocolloid, the linearized mass flux due to diffusion and thermophoresis is $\mathbf{J} = \mathbf{u}c - D\nabla c - c_0(1 - c_0)DS_T\nabla T$ [10], where S_T is the Soret coefficient. For now we neglect magnetophoretic contributions. Introducing the concentration scale $\overline{\Delta c} = c_0(1 - c_0)|S_T|\overline{\Delta T}$ yields the normalized concentration dynamics equation

$$\frac{\partial}{\partial t}c + \mathbf{u}\nabla(c - T). \quad (2)$$

The Lewis number $L = \alpha D^{-1}$, characterizing the ratio of thermal and mass diffusivities, is also very large in ferrofluids. Thus, the temperature dynamics is much faster than that of the concentration, and the magnetosolutal microconvection does not influence the distribution of temperature. We impose the temperature gradient $\text{grad}T$ and calculate $\overline{\Delta T} = \text{grad}T \cdot L$.

A non-magnetic cylinder immersed in a ferrofluid with the magnetic permeability $\mu = 1 + \chi_0$ and exposed to the uniform magnetic field creates around itself a magnetic perturbation $\delta\mathbf{H}$. In the dimensionless form (the radius of the cylinder is assumed as a length scale L),

$$\delta\mathbf{H} = \frac{\cos(\Theta)}{r^2}\mathbf{e}_r + \frac{\sin(\Theta)}{r^2}\mathbf{e}_\Theta, \quad (3)$$

where r and Θ , \mathbf{e}_r and \mathbf{e}_Θ are the cylindrical coordinates and basis vectors. Also, the characteristic scale of the magnetic field is $\overline{\Delta H} = |K_H|H_0$ and $K_H = (\mu - 1)/(\mu + 1)$. We calculate the magnetic perturbation produced by an array of non-magnetic cylinders directly from the Maxwells equations, but the result corresponds to a superposition of 2D dipoles (3).

For typical ferrofluid parameters ($S_T = 0.1\text{K}^{-1}$, $\eta = 0.001\text{Pa}\cdot\text{s}$, $D = 2 \times 10^{-11}\text{m/s}^2$, $c_0 = 0.15$, the particle diameter 8 nm, the particle spontaneous magnetization $5 \times 10^5\text{A/m}$), the external field 0.1 T and the imposed temperature gradient correspond to a temperature difference of 20 K applied across a 1-mm thick porous membrane; the magnetosolutal Rayleigh number in the vicinity of cylindrical inclusion with the radius $2\mu\text{m}$ reaches $\text{Rm}_c = 50$. This is enough to cause a significant microconvective particle transfer, and we use this value in simulations.

2. Results. We start from the initial concentration distribution $c = -x$, which corresponds to a stationary stratification created by the temperature $T = x$.

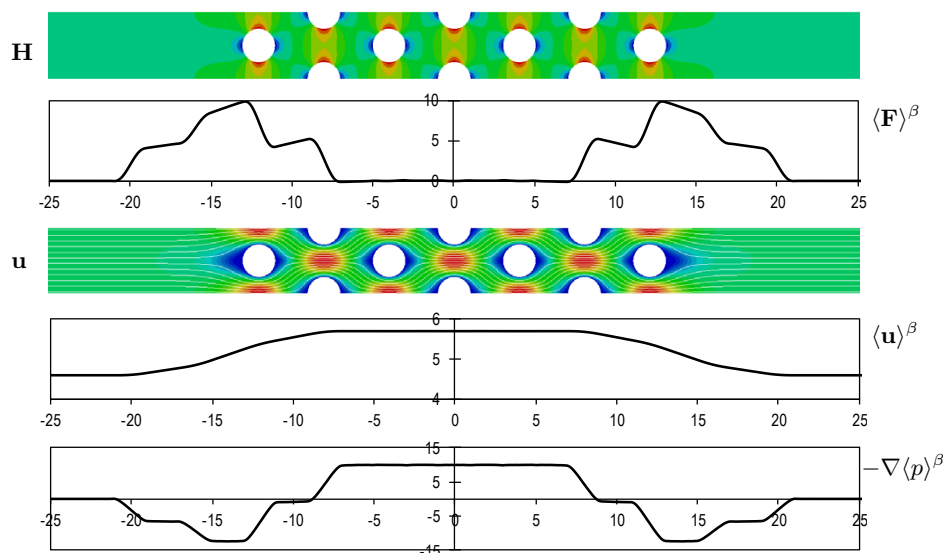


Fig. 2. Case 1 simulation ($\varepsilon = 0.8$, fixed concentration gradient); from top to bottom: perturbation of the magnetic field H , plot of the averaged magnetic force $\langle \mathbf{F} \rangle^\beta$, streamlines of the velocity \mathbf{u} , plot of the averaged velocity $\langle \mathbf{u} \rangle^\beta$, plot of the gradient of averaged pressure $-\nabla \langle p \rangle^\beta$.

We have performed two series of simulations: in the first case, we solve only the Stokes equation and the initial concentration distribution is not allowed to change (case 1). As expected, the calculated distribution of the magnetic field perturbation $H = \mathbf{h} \cdot \delta\mathbf{H}$ is highly inhomogeneous (Fig. 2) and so is the magnetic force $\mathbf{F} = \text{Rm}_c e \nabla H$. In order to reveal the macroscopic structure of the magnetic forces, we perform spatial averaging. The correct average in periodic porous structures is the cellular average across a unit cell [11], which we denote as $\langle \dots \rangle^\beta$. The superscript β indicates that the averaging is performed in the fluid phase – in the space occupied by the ferrofluid, i.e. the intrinsic average is obtained. Interestingly, the averaged magnetic force density $\langle \mathbf{F} \rangle^\beta$ vanishes in the bulk of the porous structure and remains only in the immediate vicinity of the membrane surface, reaching a sharp maximum within approximately a single period of the porous structure at both ends of the membrane. While the averaged magnetic force is well localized, its maximum value is proportional to the value of the concentration at both ends of the membrane. So, when a concentration gradient is applied across the porous membrane, the total magnetic force is proportional to the thickness of the membrane.

In the second series of calculations, we solve also the concentration equation, advancing to the stationary/quasi-stationary state (case 2). In this case, the averaged concentration gradient decreases within the porous membrane (Fig. 3) due to the change of porosity. In turn, the distribution of the averaged magnetic force becomes asymmetric with respect to the midpoint of the membrane. A component of the averaged magnetic force appears within the bulk of the membrane counteracting the pressure difference created by the forces in the vicinity of the membrane surface. These are the consequences of convective dispersion of the concentration within the porous membrane. It can be expected that in 2D membranes these effects may lead to instabilities and oscillations.

In the framework of Darcy theory, the relationship between the averaged quantities should hold in the bulk of the porous membrane [11]

$$\langle \mathbf{u} \rangle^\beta = -\frac{K}{\varepsilon} \nabla \langle p \rangle^\beta, \quad (4)$$

where K is the permeability tensor, which we calculate by solving the closure problem numerically for a unit cell [11]. In the series of calculations when the concentration gradient is fixed (case 1), the averaged magnetic force $\langle \mathbf{F} \rangle^\beta$ vanishes within the porous structure. That is why it is absent in Eq. (4).

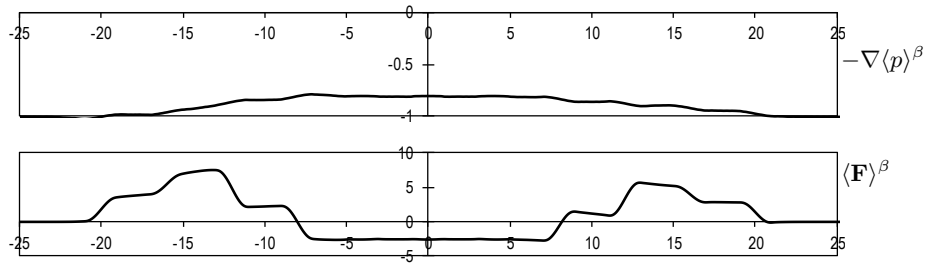


Fig. 3. Case 2 simulations ($\varepsilon = 0.8$, concentration can change); from top to bottom: plot of the gradient of averaged pressure $-\nabla \langle p \rangle^\beta$, plot of the averaged magnetic force $\langle \mathbf{F} \rangle^\beta$.

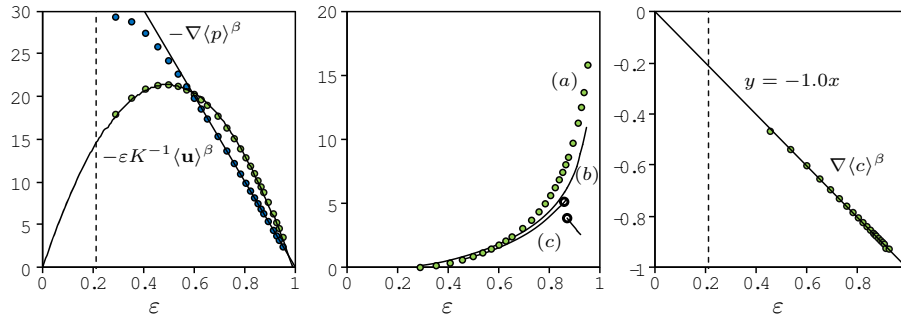


Fig. 4. Results of simulations: left: plot of $-\nabla\langle p\rangle^\beta$ and $\varepsilon K^{-1}\langle u\rangle^\beta$ for different porosities (for case 1); middle: (a) $\langle u\rangle^\beta$ (case 1), (b) $\langle u\rangle^\beta$ calculated from Eq. (4) (case 1), (c) plot of $\varepsilon^{-1}\langle u\rangle^\beta$ (case 2); right: plot of $-\nabla\langle c\rangle^\beta$ within the membrane (case 2).

The calculated quantities $\tilde{\mathbf{F}} = \varepsilon K^{-1}\langle \mathbf{u}\rangle^\beta$ and $-\nabla\langle p\rangle^\beta$ are plotted in Fig. 4 (left) with respect to the porosity ε of the membrane. While $\tilde{\mathbf{F}}$ is closely parabolic, the dependence of the averaged pressure gradient is mostly linear. Despite the difference, the Darcy law (4) acceptably captures the relationship between the averaged velocity and the pressure (Fig. 4, middle). In the second series of calculations (case 2), due to the decrease of the concentration gradient within the membrane, the averaged velocity decreases as compared with the unperturbed case (case 1). The magnitude of the concentration gradient within the membrane in this situation is proportional to the porosity ε (Fig. 4, right). Plotting the quantity $-\nabla\langle p\rangle^\beta$ (Fig. 4, middle), it corresponds to the magnitude of the averaged velocity $\langle \mathbf{u}\rangle^\beta$ in the unperturbed case (case 1). This correspondence remains up to rather large values of porosity. The little difference can be attributed to convective dispersion within the membrane.

Starting from a certain value of porosity ($\varepsilon \approx 0.85$), the dependence experiences a discontinuity, and the averaged velocity begins to decrease. This happens due to the establishing of the instability of the flow. The symmetrical configuration is replaced by the asymmetrical one and, further increasing the porosity ($\varepsilon > 0.95$), we observed periodic oscillations.

3. Conclusions. We have performed pore-scale numerical simulations of ferrofluid magnetosolutal microconvection in 1D ordered porous membranes composed of cylindrical elements. The imbalance of the concentration was created by thermophoretic separation induced by a temperature gradient. The application of the external magnetic field creates highly inhomogeneous distribution of the magnetic force within the membrane, which nevertheless possesses the well-defined macroscopic structure. A pressure difference appears across the membrane driving the flow of ferrofluid in the direction of the temperature gradient. We show that interpretation of the results of pore-scale simulations in the framework of the Darcy theory is possible, although errors as high as 30

Acknowledgements. The work has been supported by the Latvian Science Foundation, project no. 286/2012.

REFERENCES

- [1] E.YA. BLUMS. Thermomagnetophoresis of particles in a magnetic suspension. *Magnetohydrodynamics*, vol. 15 (1979), no. 1, pp. 18–22.

- [2] J.C. BACRI, A. CEBERS, A. BOURDON, G. DEMOUCHY, B.M. HEEGAARD, R. PERZYNSKI. Forced Rayleigh experiment in a magnetic fluid. *Phys. Rev. Lett.*, vol. 74 (1995), pp. 5032–5035.
- [3] K.I. MOROZOV. Gradient diffusion in concentrated ferrocolloids under the influence of a magnetic field. *Phys. Rev. E*, vol. 53 (1996), pp. 3841–3846.
- [4] M.M. MAIOROV, A.O. TSEBERS. Magnetic microconvection of the diffusion front of ferroparticles. *Magnetohydrodynamics*, vol. 19 (1983), no. 4, pp. 376–380.
- [5] D. ZABLOTSKY, A. MEZULIS, E. BLUMS. Formation of magnetoconvection by photoabsorptive methods in ferrofluid layers. *C. R. Mecanique*, vol. 341 (2013), pp. 449–454.
- [6] E. BLUMS, V. SINTS, G. KRONKALNS, A. MEZULIS. Non-isothermal separation of ferrofluid particles through grids: abnormal magnetic Soret effect. *C. R. Mecanique*, vol. 341 (2013), pp. 348–355.
- [7] E. BLUMS, V. SINTS, A. MEZULIS, G. KRONKALNS. New problems of mass transport in magnetic fluids. *Magnetohydrodynamics*, vol. 49 (2013), no. 3–4, pp. 360–367.
- [8] E. BLUMS. New transport properties of ferrocolloids: magnetic Soret effect and thermomagnetoosmosis. *JMMM*, vol. 289 (2005), pp. 246–249.
- [9] V. FRISHFELDS, E. BLUMS. Drift of ferrocolloids through a cylindrical grid by magnetic force. *J. Phys.: Condens. Matter*, vol. 20 (2008), pp. 204130.
- [10] E. BLUMS, A. CEBERS, M. MAIOROV. *Maiorov. Magnetic Fluids* (Walter de Gruyter, Berlin, New York, 1997).
- [11] M. QUINTARD, S. WHITAKER. Transport in ordered and disordered porous media I–V. *Transport in Porous Media*, vol. 14 (1994), 163–206; *Transport in Porous Media*, vol. 15 (1994), pp. 31–196.

Received 23.01.2015